THE RELATIONSHIP OF CdS/CdTe CELL BAND PROFILES TO J-V CHARACTERISTICS AND BIAS-DEPENDENT QUANTUM EFFICIENCY

Alan L. Fahrenbruch

Colorado State University, Fort Collins, CO

ABSTRACT

The built-in voltage (V_{bi}) and the charged electronic state (ES) distribution in a solar cell determine its conduction and valence band profiles.. Changes in the charge state of the ES give rise to J-V curve anomalies like cross-over, roll-over, and, in some cases, long J-V and capacitance transient effects. CdTe is highly compensated containing deep donor- and acceptor-like ES, with larger densities than the shallow acceptor density. For close compensation, the charge density in the depletion layer can be so low that V_{bi} is determined by the front and back contact work functions. In that case the cells must be analyzed in terms of an n/i/p junction model.

AMPS models of two extreme profiles are discussed here as illustrations: an n/i/p junction, where V_{bi} is mainly supported by charge at the contacts, and an n/p junction, where V_{bi} is supported by charge in the bulk CdTe within the absorber.

PATHWAYS TO INCREASED EFFICIENCY

There are several general pathways to increasing the efficiency of CdS/CdTe cells. Since J_{sc} is close to its limit, those with the most potential yield involve increasing the cell voltage at the maximum power point (V_{max}). These are discussed here in a theoretical way to view trends, allowing that they may be very difficult or impossible to realize in practice. One pathway is by increasing the net negative charge in the CdTe by "p-type doping." Another is by increasing the minority carrier lifetime (τ_n) by, for example, control of impurities, reducing growth rate, and/or changing the micro-stoichiometry. These two pathways deal with bulk materials properties. A third pathway is by decreasing the back-contact barrier height Φ_{bc} and the recombination there, both interface properties. Many other pathways are less risky and more practical including: thinner windows and/or absorber layers, increasing the window band gap, and optical optimization.

PROPERTIES OF CdTe

Although it is relatively easy to obtain high shallow acceptor densities (N_a) in single-crystal CdTe (using P, As, N, Na), it is notoriously difficult to obtain high N_a in poly-crystalline CdTe films. SIMS measurements [1,2] indicate high densities of Cl (0.01 eV donor) and Cu (0.3 - 0.4 eV acceptor) and indicate that the CdTe layer is highly compensated [3]. Since the net charge density is given by the difference between large numbers, it is quite sensitive to fabrication variables. The usual C-V measurements indicate an uncompensated shallow N_a = 1 to 4 x10^{14} cm^{-3} [4]. DLTS and admittance measurements [5] show deep trap densities considerably larger than N_a. Although there have been numerous studies of individual ES levels, attribution to specific defects remains somewhat unclear and correlation between specific ES and cell properties remains elusive.

CHARGE DISTRIBUTIONS AND MODELS

The band shapes are determined by the net fixed charge in the bulk, at the interfaces, and at the contacts. In turn, the band shapes determine the PV properties by control of recombination and by field-aided transport. The highest point in the conduction band (CB) defines a potential barrier which is a major determiner of V_{max} and V_{oc}. We examine two broadly opposite proto-typical band shapes, n/p and n/i/p, to illustrate mechanisms and trends.

If (N_a - N_d) in the CdTe layer is large and/or the CdTe is thick, the junction barrier is supported by charge stored in the n^+-TCO/n-CdS contact and in the bulk CdTe, giving an n/p junction, Fig. 1, and the built-in voltage V_{bi} is determined by the Fermi-level in the bulk CdTe.

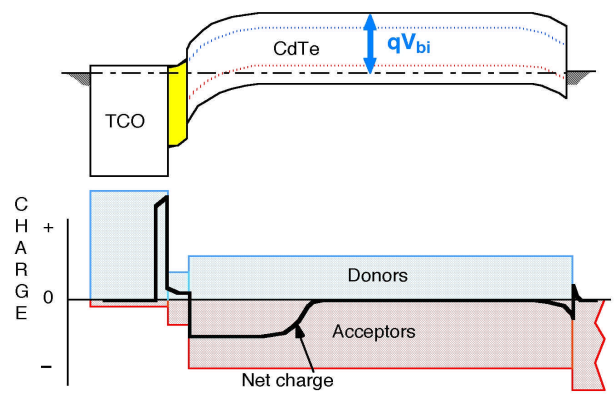

Fig. 1. Schematic of an n/p junction, based on AMPS simulation. (V_{bi} is approximate, assuming that Ef is close to the CB in the TCO).

If (N_a - N_d) in the CdTe layer is small and/or the CdTe is thin, the junction barrier is mostly supported by charge stored in the n^+-TCO/n-CdS contact and the p^+ back contact, giving an n/i/p junction, Fig. 2 and V_{bi} is determined by Φ_{bc}.

The n/i/p structure becomes more relevent with the recent trend to decreased absorber thicknesses.

Model parameters

Both models have 2 μm of CdTe with equal densities of acceptor and donor recombination centers (N_r) at mid-band-gap. For the n/i/p model, this gives a charge neutral, insulating layer. For the n/p model, shallow acceptors N_a are added and since they are shallow (E_a – E_{vb}) = 0.1 eV, they have negligible recombination. The CdS layer is 0.1 μm thick and has N_d = 10^{16} cm^{-3} shallow donors and N_{a1} =

Electron and hole surface recombination velocities at the front and back contacts are all 1e7 cm/sec for all the models

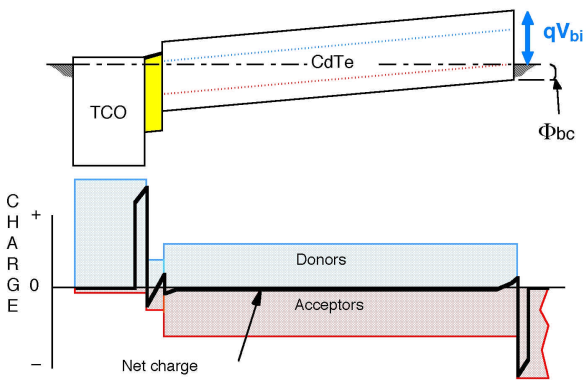

Fig. 2. Schematic of an n/i/p junction.

$5x10^{15}$ cm^{-3} acceptor-like recombination centers at mid-band-gap. In both of these models we will vary V_{bi}.

Recombination centers and minority carrier lifetime

Two alternate views of the cross-sections of recombination centers are considered here.

In the simple physical view the cross sections for electrons σ_n and holes σ_p are asymmetric: (1) a geometrical cross section for a neutral center $\approx 10^{-15}$ cm^2, and (2) a coulomb attractive cross section for a charged center with a single charge $\approx 10^{-12}$ cm^2.

On the other hand, Time Resolved Photoluminescence (TRPL) measurements in completed cells give minority carrier lifetimes (τ) values of 0.1 to 2 ns [6], with good correlation between τ_n and V_{oc}. (E.g., $\tau \approx 10^{-9}$ sec implies $\sigma \approx 10^{-12}$ cm^2 for $N_r = 10^{14}$ cm^{-3}). TRPL measures $\tau_n + \tau_p$, so τ_p < or = τ_n, and so σ_p > or = σ_n. For this paper we choose $\sigma_p = \sigma_n$ and call it the symmetric case.

- Asymmetric: N_r donor-like centers with $\sigma_n \approx 10^{-12}$ and $\sigma_p \approx 10^{-15}$ cm^2 plus N_r acceptor-like centers with $\sigma_n \approx 10^{-15}$ and $\sigma_p \approx 10^{-12}$ cm^2
- Symmetric: $N_r/2$ donor-like centers with $\sigma_n = \sigma_p \approx 10^{-12}$ cm^2 plus $N_r/2$ acceptor-like centers with $\sigma_n = \sigma_p \approx 10^{-12}$ cm^2

In both cases the extremum (all centers empty) minority carrier lifetime for electrons is $\approx 10^{-9}$ sec for $N_r = 10^{14}$ cm^{-3}, but in the asymmetric case the effective SRH lifetime is much larger. Despite their seeming similarity, the models give very different results for the two choices. We treat the asymmetric case first.

n/i/p model

For the n/i/p model V_{bi} is varied by changing the back-contact barrier height Φ_{bc}. The J-V curves, Fig. 3, show that V_{oc} scales almost linearly with decreasing Φ_{bc} and that J_{sc} and ff remain relatively constant.

In Fig. 4 the efficiency (Eff) increases almost directly with a decrease in Φ_{bc} and most of the increase is due to Voc. For $N_r \sim 10^{13}$ to 10^{14}, Eff is relatively insensitive to N_r. AMPS n/i/p models using these values give good agreement with measured J-V curves. phi, bc ~ 0.35 eV

Some general signatures of the n/i/p profile resulting from back-contact barrier changes and small net carrier density in the insulating layer are:

- V_{oc} shifts with Φ_{bc} changes, with J_{sc} and ff relatively constant,
- The decrease of Apparent Quantum Efficiency (AQE) with increasing dark, forward bias is uniform over wavelength (λ),
- Capacitance (C)is relatively constant with applied bias,
- Transients and hysteresis occur in C, J-V, and AQE with changes in illumination and/or bias.

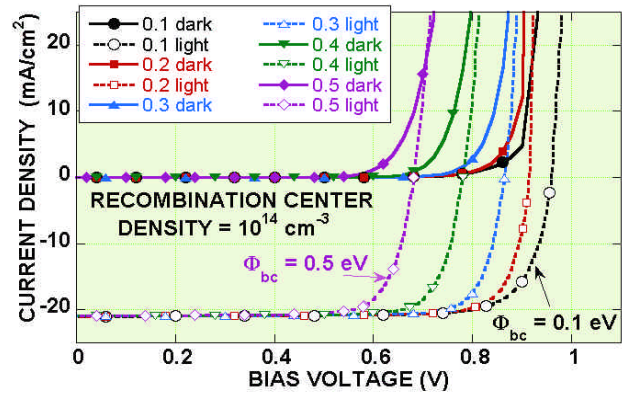

Fig. 3. J-V curves for the asymmetric case. For good, experimental cells F_{bc} = 0.3 – 0.4 eV is reasonable. cases: p-i-n 0.x 1eyr z x = 1,2,3,4,5 y = 13,14,15

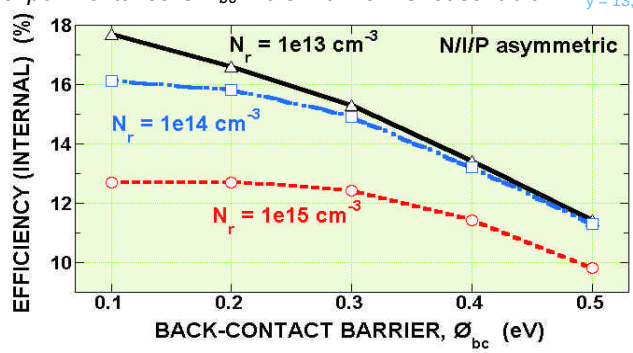

Fig. 4. Efficiency vs F_{bc} data for the asymmetric case.

n/p model

For the p/n model V_{bi} is varied by changing the net charge in the CdTe by introducing shallow acceptors at 0.1 eV above valence band. Φ_{bc} is set at 0.2 eV here. V_{oc} is generally higher than for the n/i/p model and there is a trade off between V_{oc} and ff and J_{sc}, Fig. 6.

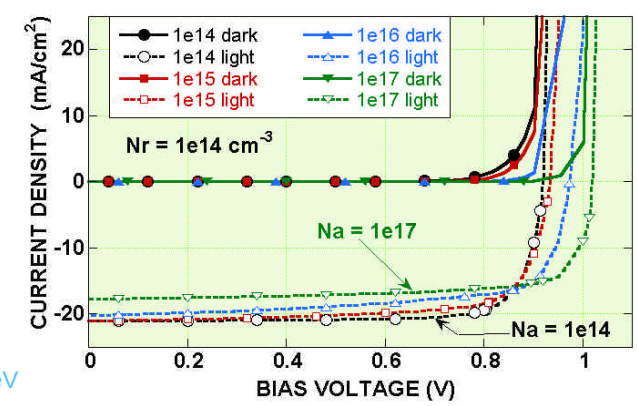

Fig. 5. J-V curves vs N_a for the n/p asymmetric case. For good experimental cells N_a-$N_d \approx 3x10^{14}$ cm^{-3} is reasonable.

The efficiency goes down for increasing N_a, due to ff loss and is quite sensitive to N_r throughout the range, Fig. 6.

Some general signatures of the n/p junction are:

should be 1e15

should be 1e14

- V_{oc} increases while ff and J_{sc} decrease with processing,
- AQE decreases mainly at long λ with forward bias.

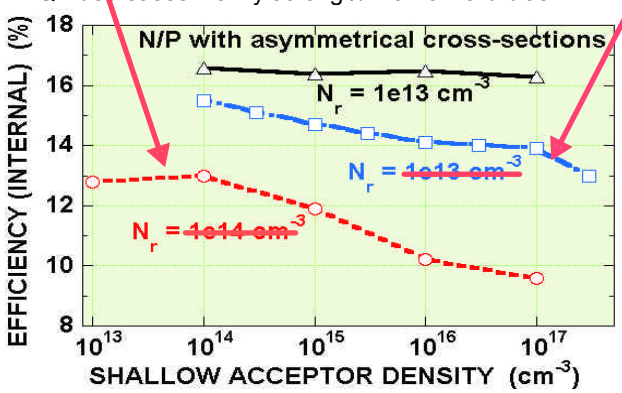

Fig. 6. Efficiency vs N_a for the n/p asymmetric case.

- C varies normally with applied bias,
- C-V, J-V and AQE are relatively insensitive to illumination and/or bias, and
- For high Φ_{bc}, the roll-over above V_{oc} due to the series Schottky voltage drop is similar in dark and light.

Since the n/i/p configuration provides excellent current collection but moderate voltage, and the n/p configuration provides higher voltage, the optimum configuration is to have the front part of the CdTe insulating and the back part highly doped.

COMPARISON OF ASYMMETRIC AND SYMMETRIC CROSS SECTION RESULTS

Using equal cross-sections for electrons and holes gives a very different results. For the n/i/p junctions of Fig. 7, both with $\tau_n = 10^{-9}$ cm^2, the shapes of the curves are quite similar, but the symmetric case efficiencies are less than half of those for the asymmetric case.

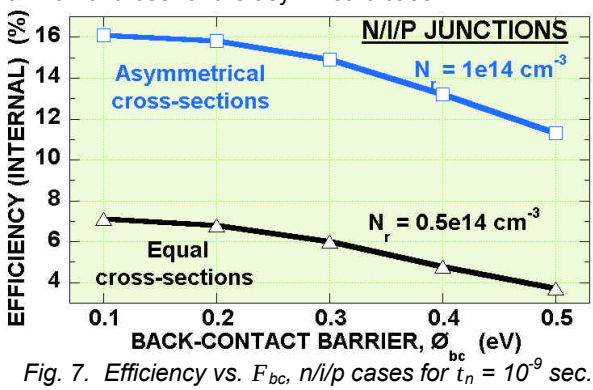

Fig. 7. Efficiency vs. F_{bc}, n/i/p cases for $t_n = 10^{-9}$ sec.

For the n/p junctions (Fig. 8), the efficiencies for both cases approach 14% for higher shallow acceptor densities. These data show that increasing acceptor density <u>decreases</u> efficiency for the asymmetric assumption, but <u>increases</u> efficiency for the equal cross-section assumption. These differences arise from how Shockley-Read-Halll recombination is affected by asymmetries. The proper choice is obviously critical to modeling, but unclear at this time and there remains an apparent paradox. The asymmetric n/i/p AMPS models, using measured values for N_a and Φ_{bc} are consistent with measured J-V data. However, TRPL lifetime measurements are consistent with measured V_{oc} values but not with AMPS models.

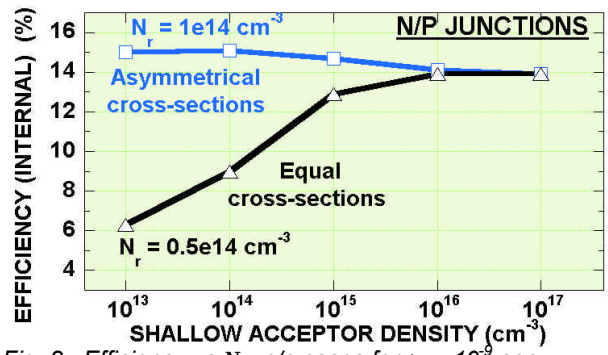

Fig. 8. Efficiency vs N_a, n/p cases for $t_n = 10^{-9}$ sec.

IMPLICATIONS FOR MEASUREMENT AND CHARACTERIZATION

The first (and easiest) hurdle in modeling a device is duplicating the general features of the J-V curves in light and dark. In general, it is considerably simpler to obtain experimental V_{oc} and ff value pairs using the n/i/p structure. With the n/p structure, V_{oc} is consistently too high for a given ff value. It is likely that the real device is somewhere between these two extremes, but very little about the band profiles can be learned from fourth quadrant J-V curves. Many different measurements must be satisfied by a valid model and completing the link between the models and the TRPL lifetime is one such test.

Although the band shapes are critically important they cannot be measured or observed directly. Modeling has been very successful at explaining certain aspects of cell behavior such as roll-over [7,8], anomalous AQE(V) [9,10], and photoconductivity in the CdS [11] and thus describing parts of the band profiles. However, a clearer description of lifetime and more quantitative capture cross section data is needed for accurate modeling of the whole device.

Present methods for constructing band profiles are indirect. Capacitance-admittance spectroscopies, although complex and difficult to interpret, yield information about deep states [5]. Longer term transients in the capacitance [12] and forward bias current [13] point to the importance of photo-conductivity in the CdTe layer. UPS and XPS have been used to determine the interface charging and dipole potentials in the CdS/CdTe cell, but determination of accurate band profiles in the bulk CdTe is difficult [14].

Methods not yet used on CdTe, include holographic TEM which has been used to determine the band offset potentials at buried interfaces in InGaN quantum wells [15]. Internal photoemission has shown considerable success in direct determination of contact barrier heights in various metal/semiconductor junctions [16], so it offers an independent measurement of Φ_{bc} in CdTe.

<u>Focus on AQE(V)</u>

Changes in quantum efficiency with bias voltage in dark and light have been major testing grounds for modeling, beginning with many studies aimed at explaining light/dark cross-over of J-V curves [11] and then expanding to AQE and AQE(V). Batzner et al. [9] observed negative AQE and |AQE| > 1 for dark forward bias (Fig. 9). Subsequent modeling by Gloeckler et al [10] has explained all these unique features by photo-gating of dark forward-bias current by the CdS layer and photo-modulation of back-contact saturation current at the back of the cell, using rather simple AMPS models.

Gloeckler's AMPS models are equivalent to dc measurements

These lock-in amplifier data (typically 200-300 Hz) are small-signal *ac* measurements, assuming a linear cell response and the phase shift (~ 110°) is interpreted as a negative AQE.

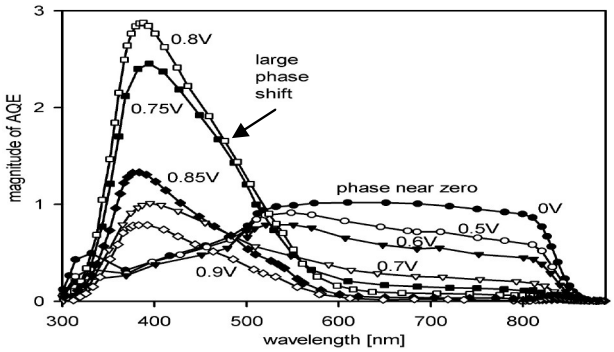

Fig. 9. Dark AQE curves for various bias voltage [9].

The uncertainty in the interpretation of the phase shift can be removed using direct *dc* measurements of AQE with LED sources to view the whole waveform as the light is turned on and off [17], Fig. 10. At low bias, *dc* AQE gives positive values, with well-shaped steps in good agreement with the ac measurements. However, at high forward bias (> V_{max}), the AQE becomes negative and slow transients for both red (630 nm) and blue (430 nm) light are seen. These slow transients are too complex to be measured with ac techniques.

470 nm

The decay curves seen in the dark for both red and blue show that previous light exposure affects the dark transport for 10s of seconds and demonstrate that the cell current cannot be considered as the sum of dark and light currents.

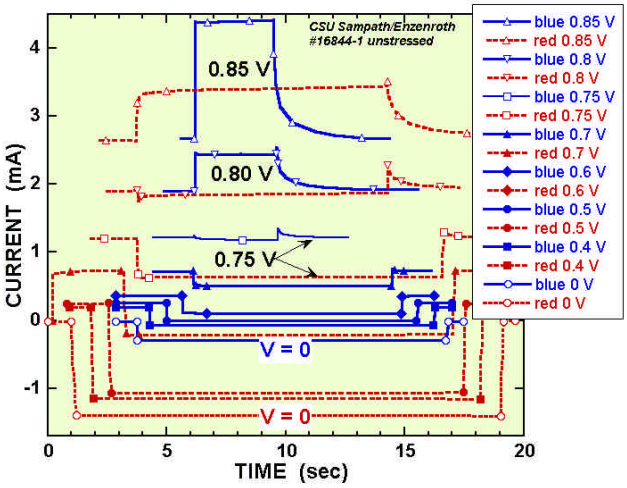

Fig. 10. dc AQE. The first step is the dark dc bias current response to a constant voltage supply, followed by a light pulse ~ 5 to 10 sec long. Red (blue) Jsc values are 4.9 (1.0) mA/cm^2.

The transient structure in the red response (100% being absorbed in the CdTe) along with negative AQE values suggests photoconductivity in the CdTe. Doing this experiment as a function of temperature might be used to determine deep state energy levels involved in transport. The end-states of the transient measurements were successfully modeled with AMPS using $N_d = 10^{16}$ donors in the CdS at E_{cb} - 0.1 eV and $N_a = 2x10^{16}$ acceptors at E_{vb} + 0.7 eV. For the acceptors, $\sigma_n = 10^{-18}$ cm^2 and $\sigma_p = 10^{-12}$ cm^2, so that blue light "electronically dopes" the CdS, making it more negative and reducing the barrier to give the photo-gating effect. Cells from other makers show well shaped steps to about 1 V bias, but the negative AQE for red and blue is still present at high forward bias.

CONCLUSIONS

The band diagrams of real cells are still unclear but emerging. Modeling has had good success in explaining specific aspects of cell behavior (roll-over, negative AQE, CdS photoconductive effects). However, more rigorous descriptions of lifetime and more quantitative capture cross section data is needed for accurate modeling of the whole device.

The asymmetric cross-section model suggests an emphasis on controlling Φ_{bc} to increase efficiency, while the symmetric model predicts increasing N_a to be the best approach.

Direct-current measurement of AQE(V) agrees with *ac* methods for biases up to ~ V_{max}. Above that the transient waveforms produced by light steps are too complex to measure with ac methods. Dark transport is substantially altered by previous light exposure and photoconductive effects were observed in both CdS and CdTe.

REFERENCES

1 S. Asher et al., ***28th*** *IEEE PVSC* (2000) p. 479.

2 M. Emziane et al. Semicond. Sci. Technol. **20**, 434 (2005)

3 Y. Marfaing, Thin Solid Films **387**, 123 (2001).

4 J.R. Sites, Annual Report to NREL, Aug. 2002, "Device Physics of Thin Film Polycrystalline Cells..," Colorado State University, p. 9.

5 A.S. Gilmore et al., ***29th*** *IEEE PVSC* (2002) p. 604, and V. Komin et al., ***28th*** IEEE PVSC (2000) p.676.

6 W. Metzner, NCPV CdTe Team Meeting, 3/9/2006.

7 T. McMahon and A. Fahrenbruch, **28th** IEEE PVSC (2000) p. 539.

8 J. R. Sites et al., NCPV CdTe Team Meeting, May 5 (2005)

9 D.L. Batzner et al., Mat. Res. Soc. Symp. Proc. **668**, H5.17 (2001)

10 M. Gloeckler and J.R. Sites, *J. Appl. Phys.* **95**, 3845 (2004)

11 S. Hegedus, Prog. Photovolt. **5**, 151 (1997) and Mat. Res. Soc. Symp. Proc. **763**, B9.5.1 (2003).

12 F. Seymour et al., ***31th*** *IEEE PVSC* (2005) p.275

13 A. Fahrenbruch, Mat. Res. Soc. Symp. Proc. **865**, F12.1 (2005)

14 J. Fritsche et al. Thin Solid Films **403**, 252 (2002) and W. Jaegermann et al., Mat. Res. Soc. Symp. Proc. **865**, F6.1.1 (2005)

15 J. Cai and F. Ponce, J. Appl. Phys. 91, 9856 (2002).

16 C.S. Yu et al., Appl. Phys. Lett. **73**, 3917 (1998).

17 A. Fahrenbruch, NCPV CdTe Team Meeting, March 9 (2006).